



## ARTICLE OPEN

# Epigenetic aging is accelerated in alcohol use disorder and regulated by genetic variation in *APOL2*

Audrey Luo<sup>1</sup>, Jeesun Jung<sup>1</sup>, Martha Longley<sup>1</sup>, Daniel B. Rosoff<sup>1</sup>, Katrin Charlet<sup>1,2</sup>, Christine Muench<sup>1</sup>, Jisoo Lee<sup>1</sup>, Colin A. Hodgkinson<sup>3</sup>, David Goldman<sup>3</sup>, Steve Horvath<sup>4,5</sup>, Zachary A. Kaminsky<sup>6</sup> and Falk W. Lohoff<sup>1</sup>

To investigate the potential role of alcohol use disorder (AUD) in aging processes, we employed Levine's epigenetic clock (DNAm PhenoAge) to estimate DNA methylation age in 331 individuals with AUD and 201 healthy controls (HC). We evaluated the effects of heavy, chronic alcohol consumption on epigenetic age acceleration (EAA) using clinical biomarkers, including liver function test enzymes (LFTs) and clinical measures. To characterize potential underlying genetic variation contributing to EAA in AUD, we performed genome-wide association studies (GWAS) on EAA, including pathway analyses. We followed up on relevant top findings with in silico expression quantitative trait loci (eQTL) analyses for biological function using the BRAINEAC database. There was a 2.22-year age acceleration in AUD compared to controls after adjusting for gender and blood cell composition ( $p = 1.85 \times 10^{-5}$ ). This association remained significant after adjusting for race, body mass index, and smoking status (1.38 years,  $p = 0.02$ ). Secondary analyses showed more pronounced EAA in individuals with more severe AUD-associated phenotypes, including elevated gamma-glutamyl transferase (GGT) and alanine aminotransferase (ALT), and higher number of heavy drinking days (all  $ps < 0.05$ ). The genome-wide meta-analysis of EAA in AUD revealed a significant single nucleotide polymorphism (SNP), rs916264 ( $p = 5.43 \times 10^{-8}$ ), in apolipoprotein L2 (*APOL2*) at the genome-wide level. The minor allele A of rs916264 was associated with EAA and with increased mRNA expression in hippocampus ( $p = 0.0015$ ). Our data demonstrate EAA in AUD and suggest that disease severity further accelerates epigenetic aging. EAA was associated with genetic variation in *APOL2*, suggesting potential novel biological mechanisms for age acceleration in AUD.

*Neuropsychopharmacology* (2020) 45:327–336; <https://doi.org/10.1038/s41386-019-0500-y>

## INTRODUCTION

Excessive alcohol use is a major risk factor for premature death worldwide and is associated with an increased risk for aging-related diseases, such as diabetes, myocardial infarction, liver diseases, and cancer mortality [1–3]. Research studies have shown that individuals with alcohol use disorder (AUD) die earlier than healthy individuals, and they are at a significantly increased risk for all-cause mortality [4, 5]. Furthermore, heavy alcohol consumption in healthy individuals has previously been shown to be associated with increased rates of aging [6, 7]. Although the negative impact of alcohol use on lifespan and health-span as well as the potential influence of AUD on aging processes have been reported, the relationship between accelerated aging and AUD severity and the underlying biological process have not been well investigated.

One way to further characterize biological age in contrast to chronological age is the use of epigenetic clocks, which are hypothesized to capture molecular processes involved in declining tissue function [8]. The weighted average of methylation levels at specific age-associated cytosine phosphate guanines (CpG) sites

are used to calculate DNA methylation age (DNAm age). DNAm ages may be more promising markers to predict aging because they indicate changes in transcriptional programs and can reflect cumulative effects of exposures, for instance to alcohol, over time. Given that individuals with AUD have been shown to have differential methylation levels compared to healthy controls (HC) [9–11], epigenetic clocks could capture how changes in methylation patterns in individuals with AUD are associated with changes of DNAm age, allowing for the investigation into the shared molecular mechanisms underlying alcoholism and aging.

Different generations of the epigenetic clocks provide different measures and characteristics of epigenetic aging. Horvath and Hannum epigenetic clocks (first generation) were designed for the Illumina 450K methylation array and used chronological age to select for the CpG sites in their approaches. On the other hand, Levine clock was recently developed and designed for all three Illumina array platforms (27K, 450K, and EPIC 850K chips) with whole blood [12]. Levine's approach first calculated the phenotypic age, a composite representing death and disease risk and predicting physiological dysfunction. The phenotypic age

<sup>1</sup>Section on Clinical Genomics and Experimental Therapeutics, National Institute on Alcohol Abuse and Alcoholism, National Institutes of Health, Bethesda, MD, USA; <sup>2</sup>Department of Psychiatry and Psychotherapy, Charité – Universitätsmedizin Berlin, Berlin, Germany; <sup>3</sup>Laboratory of Neurogenetics, National Institute on Alcohol Abuse and Alcoholism, National Institutes of Health, Bethesda, MD, USA; <sup>4</sup>Department of Human Genetics, David Geffen School of Medicine, University of California Los Angeles, Los Angeles, CA, USA; <sup>5</sup>Department of Biostatistics, Fielding School of Public Health, University of California Los Angeles, Los Angeles, CA, USA and <sup>6</sup>The Royal's Institute of Mental Health Research, University of Ottawa, Ottawa, ON, Canada

Correspondence: Falk W. Lohoff (falk.lohoff@nih.gov)

These authors contributed equally: Audrey Luo, Jeesun Jung

Received: 20 June 2019 Revised: 6 August 2019 Accepted: 12 August 2019

Published online: 29 August 2019

is predicted by a linear combination of chronological age and select clinical characteristics (e.g., albumin, creatinine, white blood cell count, and others). Levine's algorithm then estimated the epigenetic age using the selected DNA methylation CpG sites that predicted the phenotypic age. The Levine DNAm PhenoAge clock has been garnering attention for its ability to predict aging outcomes and aging-related diseases risks, including all-cause mortality [12]. Different epigenetic clocks may capture different aspects of aging, and a growing body of literature suggests that it may be advantageous to examine multiple clocks with alcohol-related phenotypes.

A measure of epigenetic age acceleration (EAA), defined as DNAm age-adjusted for chronological age, is calculated by taking the residual resulting from regressing DNAm age on chronological age [8, 12–14]. EAA in blood and brain tissues has been linked to cognitive functioning, Parkinson's disease, menopause, Alzheimer's disease, and Down syndrome. There are only a few studies available that investigate the effect of alcohol on EAA. Using Horvath's 2013 clock, we have previously shown that excessive alcohol consumption and a diagnosis of alcohol dependence were associated with EAA across different tissues, including blood and liver [15]. Furthermore, heritability of EAA in blood is high ( $h^2 \approx 0.4\text{--}0.5$ ), which is consistent with pedigree- or twin-based studies and EAA differs across racial groups [8, 16, 17], but little is known about the genetic architecture underlying EAA in individuals with AUD.

In this paper, we first aimed to confirm the relationship between AUD diagnosis and accelerated epigenetic aging in the largest AUD cohort currently available. In particular, we investigated how AUD severity, characterized by abnormal liver function and number of heavy drinking days, is associated with age acceleration using the Levine EAA, as well as the Horvath and Hannum EAA [12]. The secondary purpose of our study was to perform a genome-wide association study (GWAS) of DNAm age in individuals with AUD to identify genetic contributions to EAA. Furthermore, we aimed to investigate the genetic mechanism underlying age acceleration and AUD by conducting a cis-expression quantitative trait loci (eQTL) study using the archived eQTL dataset in the BRAINEAC database. Subsequently, we performed a gene set enrichment analysis using Meta-Analysis Gene-set Enrichment of variant associations (MAGENTA) to identify biologically relevant pathways that are enriched by genes harboring significant variants.

## MATERIALS AND METHODS

### Study participants

The sample consisted of 532 participants (331 AUD and 201 HC). All participants provided a blood sample which was used for genome-wide DNA methylation analysis and clinical marker collection, including the liver function tests for gamma-glutamyl transferase (GGT), alanine aminotransferase (ALT), aspartate aminotransferase (AST), and alkaline phosphatase (ALP). Participants completed the Structured Clinical Interview for Diagnostic and Statistical Manual of Mental Disorders (DSM)-IV-TR (SCID-IV) to determine alcohol dependence diagnosis. A diagnosis of alcohol dependence in the DSM-IV is equivalent to moderate to severe AUD diagnosis according to the DSM-5 with a concordance of 93% [18]. Participants also completed self-report questionnaires, including the Timeline Followback (TLFB), a measure of alcohol intake over the previous 90 days [19], and the Fagerström test for nicotine dependence (FTND) [20]. All participants completed screening assessments where information on their demographics, recent drinking history, and exposure to early life stress was collected. Data on family history of alcohol use was not collected. Study participants were recruited to the National Institute on Alcohol Abuse and Alcoholism (NIAAA) at the National Institutes of Health (NIH), USA. All participants provided informed written

consent in accordance with the Declaration of Helsinki and were compensated for their time. The study was approved by the Institutional Review Board of the NIAAA.

### DNA methylation measurements in peripheral blood

DNA methylation levels from whole blood samples were assessed using an Infinium MethylationEPIC BeadChip microarray (Illumina Inc., San Diego, California) according to the manufacturer's protocol. The waterRmelon package in R was used to process the raw data. After cross-reactive probes and probes that failed quality assessment were removed, a scale-based correction was applied for Illumina type I relative to type II probes. We used a quantile normalization approach to make methylated and unmethylated intensity values identical and then quantified the  $\beta$ -value using the ratio of intensities between methylated and unmethylated alleles [21]. The residuals of a linear model of  $\beta$ -values as a function of sodium bisulfite modification batch were taken to adjust the values. Measures of blood cells counting for 6 cell types (granulocytes, monocytes, natural killer cells, B cells, CD4+ T cells, and CD8+ T cells) were obtained based on the Houseman estimation method [22]. The dataset consisted of  $\beta$ -values for 835 928 CpG sites in 532 individuals.

### Calculating DNAm age and age acceleration

Three epigenetic clocks utilizing different algorithms, and CpG sites were employed to estimate DNAm age [8, 12–14]. DNAm age was calculated as the weighted average of selected CpG sites according to the coefficients reported in each epigenetic clock. Hannum's clock used an approach based on 71 CpG sites and was made for adult blood samples; Horvath's 2013 clock was a multi-tissue predictor of age, using 353 CpG sites; and lastly, Levine's DNAm PhenoAge clock employed 513 CpG sites selected based on phenotypic age, which was a measure representing the expected age that corresponded to a person's estimated hazard of mortality as a function of his/her biological profile. Where Hannum's and Horvath's 2013 clocks were optimized for Illumina 27k and 450k chips, Levine's clock used CpG sites available on all three chips (27k, 450k, EPIC). Seventeen of the 353 CpGs and 6 of the 71 CpGs necessary to calculate epigenetic age using the Horvath and Hannum methods, respectively, were missing. Horvath's algorithm imputed the missing CpG sites, whereas the missing probes were excluded from the epigenetic age calculation in Hannum's clock. EAA was then estimated by taking the residual resulting from regressing DNAm age on chronological age. A positive EAA represents a positive deviation from chronological age in years and indicates accelerated aging, whereas a negative EAA indicates younger biological age compared to chronological age, or decelerated aging.

### Statistical analysis

To examine differences in epigenetic aging in AUD and controls, a linear regression model was used with EAA, satisfying normality (by Shapiro-Wilk test,  $p > 0.05$ ), as a dependent variable and AUD diagnosis as an independent variable with gender and blood-cell type composition as covariates (basic model). The fully adjusted model included additional covariates for race, smoking status, and body mass index (BMI). Race, as determined by ancestry-informative markers score (AIMs), was included because race/ethnicity has previously been shown to be associated with epigenetic aging [23]. Smoking status was included to account for potential confounding lifestyle factors affecting aging due to the disproportionately high concurrence of smoking in the AUD individuals compared to HCs groups [24]. Furthermore, BMI has previously been shown to predict accelerated epigenetic aging [25]. Blood-cell counts were included as covariates to correct for differences in blood cell-type composition between individuals [26, 27].

For exploratory analyses, additional linear regression models that were adjusted for all covariates were used to examine the relationship between EAA and the number of heavy drinking days in a 90-day window ( $\geq 4$  drinks a day for females;  $\geq 5$  drinks a day for males) within individuals with AUD. To further dissect the AUD phenotype, we examined EAA in the most and least severe cases defined by the third (highest) quartile and the first (lowest) quartile of each respective biomarker level (GGT, ALT, AST, and ALP level) in the AUD group. Linear regression models were used to compare the EAA between samples in the highest and lowest quartiles of each biomarker. Statistical analyses were performed in R version 3.5.1.

#### GWAS analysis for epigenetic age acceleration

A genome-wide association study (GWAS) was performed in European Ancestry (EA) and African Ancestry (AA) participants separately with the Illumina OmniExpress and Illumina OmniExpressExome BeadChips (Illumina, San Diego, CA). Ethnicity for each individual was characterized using a panel of 2500 AIMs, which were then compared to the 51 worldwide populations represented in the Human Genome Diversity Cell Line Panel of the Human Genome Diversity Project (HGDP) and Centre d'Etude du Polymorphisme Humain (CEPH), which includes 1051 individuals (<http://www.cephb.fr/HGDP-CEPH-Panel>) [28]. Ancestry scores were calculated using Structure, version 2.2 (<https://web.stanford.edu/group/pritchardlab/structure.html>) where data for the CEPH diversity panel were run along with our samples using the AIMs [29]. The ancestry scores for six ethnic factors (Africa, Europe, Asia, Far East Asia, Oceania, and Americas) were then estimated for each subject. Based on the 6 ethnic AIM scores, we identified EA by having a European AIM score of 80% or greater and AA participants by having an African AIM score of 20% or greater and AIM scores for other races of 5% or lower.

Based on the genetically identified EA and AA individuals, we conducted a series of quality control (QC) procedures within each race group including: sex check by X chromosome, Hardy–Weinberg equilibrium (HWE) test in a control sample in EA and AA separately ( $P > 0.0001$ ), missingness by SNP (missing rate  $< 0.01$ ) and missingness by subjects (missing rate  $< 0.03$ ), and minor allele frequency (MAF) over 1%. The final sample size for the GWAS analyses after QC procedure was 256 in EA and 230 in AA. The total number of SNPs tested for in the GWAS with EAA was 613 209 for EA and 666 531 for AA.

A linear regression with an additive genetic model was utilized to test for the association between each SNP and Levine's EAA in AUD group after adjusting for gender, smoking status, and blood cell-type composition as covariates. All analyses were performed in AUD EA ( $n = 154$ ) and AUD AA ( $n = 156$ ) separately. We then carried out a fixed-effects meta-analysis weighted by inverse variance using the GWAS results of EA AUD and AA AUD samples. SNPs that had substantial heterogeneity across the two GWAS results (Cochran's Q-test  $p$ -value  $< 0.05$  and heterogeneity index  $I^2 > 75$ ) were removed. The total number of SNPs for the genome-wide meta-analysis was 494 067. The threshold for the GWAS significant SNPs was  $7.5 \times 10^{-8}$  ( $= 0.05/666\ 531$ ) determined by a Bonferroni Correction that used the number of SNPs tested in AA sample. All genetic analyses were conducted using PLINK 1.90 software.

#### Pathway analyses using MAGENTA

To illustrate potential biological processes that influence epigenetic age acceleration in AUD, we explored the data in several ways. First, using the results of the genome-wide meta-analysis, we carried out Meta-Analysis Gene-set Enrichment of variant associations (MAGENTA) analysis to identify biological pathways that are enriched for genes having significant variants [30]. Twenty pre-specified biological pathways and their associated gene sets were extracted from the KEGG pathway database [31]

(Supplementary Table S1). After extending gene boundaries to  $\pm 50$  kb, we assigned SNPs to each gene and corrected for gene size, variant number, and linkage disequilibrium (LD). We then performed gene set enrichment analysis (GSEA) in the MAGENTA with 95th and 75th percentiles, which were the default parameter values for a highly polygenic trait. The empirical nominal  $p$ -values were estimated based on 10 000 permutations. False discovery rate (FDR) adjusted  $p$ -values were calculated using MAGENTA.

#### In silico functional analyses

*APOL2* is highly expressed in neurons of the human hippocampus ([www.proteinatlas.org](http://www.proteinatlas.org)) [32]. Given that *APOL2* was our top finding and that it is expressed in several brain regions, we performed cis-expression quantitative trait loci (eQTL) analysis for *APOL2* to identify a correlation between the genetic variants and expression level in the brain tissues at both the specific exon level and the transcript level using the brain expression quantitative trait loci (eQTL) Almanac (BRAINEAC) database, which includes either exon-level or gene-level data across 10 brain regions from 134 neurologically normal EA subjects [33].

## RESULTS

Epigenetic aging was studied in AUD and HC. Sample characteristics are described in Supplementary Table S2. The mean age of the sample was 40.7 years ( $SD = 12.5$ ) and 44.3% of the sample was female. AUD and HC differed significantly in chronological age ( $p < 0.0001$ ), with AUD being older than the controls. The AUD group had a higher proportion of smokers ( $p < 0.0001$ ) and males ( $p = 0.04$ ) and greater average BMI than the controls ( $p = 0.01$ ).

#### Accelerated epigenetic aging in AUD

EAA derived from Levine's DNAm PhenoAge clock was significantly higher in AUD cases compared to healthy controls before adjusting for covariates ( $b = 2.7$ ,  $p = 1.6 \times 10^{-7}$ ). After adjusting for gender and blood cell composition in the basic model (Fig. 1a, Table 1), age acceleration in AUD cases remained significant ( $p = 1.85 \times 10^{-5}$ ). Individuals with AUD were on average 2.22 years older than HC, with an overall mean positive EAA (accelerated aging) in AUD cases (0.84 years) and mean negative EAA (decelerated aging) in controls (1.38 years). When adjusted for additional covariates in the full model, age acceleration in individuals with AUD compared to controls was slightly lower than in the basic model ( $b = 1.38$ ,  $p = 0.02$ ), but still significant. Levine DNAm age was highly correlated with chronological age in both AUD and HC (Fig. 1b), as were DNAm ages derived from other epigenetic clocks. Positive smoking status ( $b = 1.81$ ,  $p = 0.001$ ) and blood cell composition (monocytes:  $b = 60.0$ ,  $p = 0.04$ ; granulocytes:  $b = 62.4$ ,  $p = 0.03$ ) demonstrated significant associations with Levine EAA in the fully adjusted model. However, we did not observe any significant difference in age acceleration between AUD and HC using the Horvath and Hannum clocks (Table 1).

Associations of drinking patterns and clinical markers on EAA In the AUD group, Levine's EAA was positively associated with the number of heavy drinking days and more severe AUD phenotypes, as measured by elevated liver enzymes (ALT, ALP, and GGT) after adjusting for covariates (Fig. 1, Table 2). In the basic model, AUD cases in the highest quartile of heavy drinking days ( $= 90$  heavy drinking days) exhibited on average 2.18 years of age acceleration ( $p = 0.01$ ) compared to AUDs in the lowest quartile of heavy drinking days ( $\leq 44$  heavy drinking days).

Exploratory analyses revealed an association of elevated GGT, ALT, and ALP levels with EAA (Table 2). Elevated levels of these clinical markers, which indicates liver damage and a more severe AUD phenotype, predicted accelerated epigenetic age. After outliers defined by  $\pm 3$  standard deviations from the mean

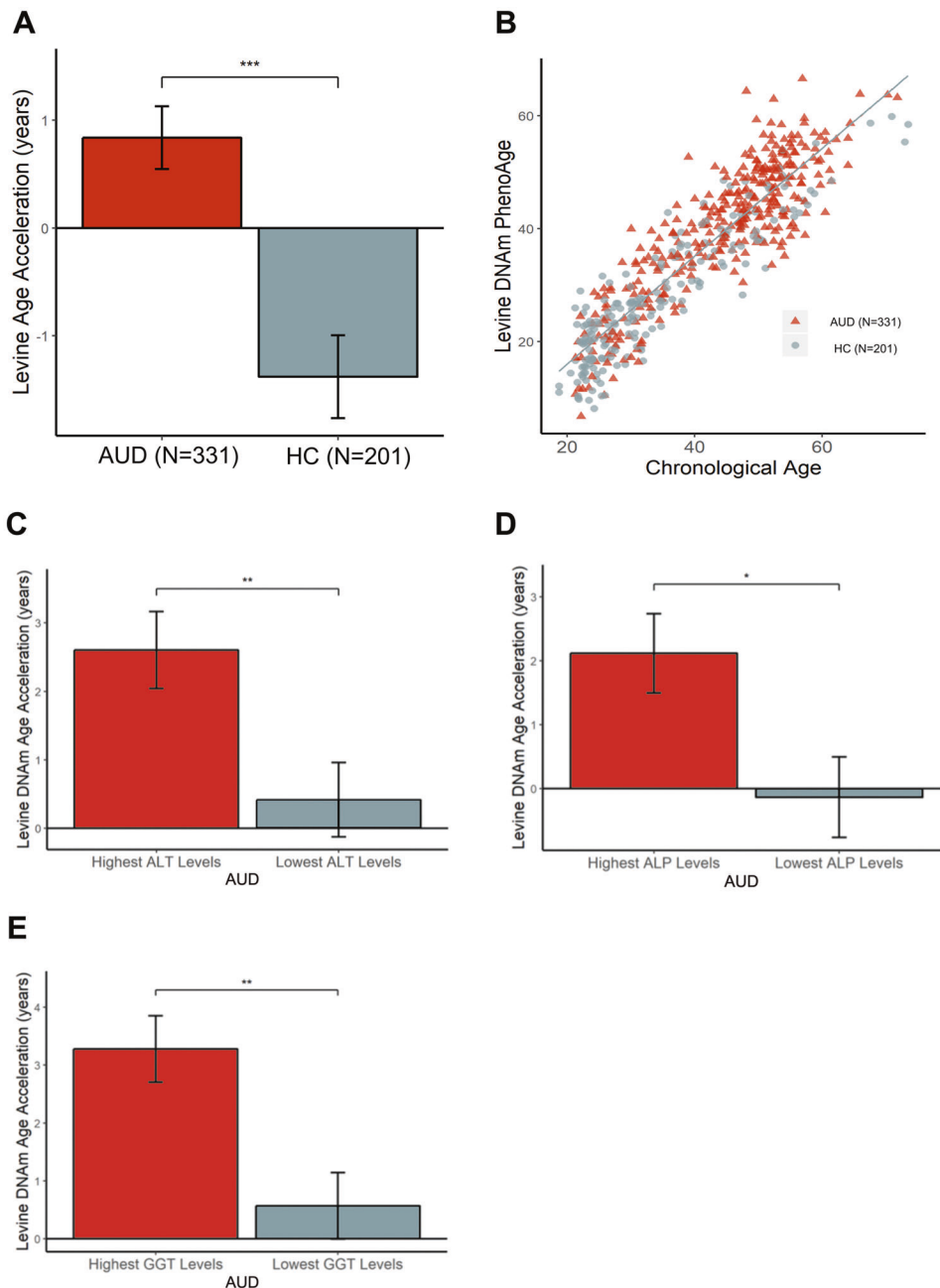


**Fig. 1** Epigenetic age acceleration in AUD. The bar plots show estimated means of age acceleration adjusted for gender and blood cell composition (basic model), as calculated from Levine's DNAm PhenoAge, and standard error (SE). **a** Age acceleration differed significantly ( $p < 0.0001$ ) between AUD cases and healthy controls. **b** The scatterplot shows the chronological age versus DNA methylation age and the line in which DNA methylation age was regressed on chronological age. Epigenetic age was highly correlated with chronological age in both groups (Levine: AUD group [ $N = 331$ ]:  $r = 0.86$ ,  $p < 0.0001$ ; control group [ $N = 201$ ]:  $r = 0.91$ ,  $p < 0.0001$ ). Points lying above the regression line indicate positive age acceleration, and points lying below the regression line indicate negative age acceleration. **c–e** Age acceleration differed significantly between AUD cases in the highest and lowest quartiles with ALT ( $p = 0.007$ ), ALP ( $p = 0.01$ ), and GGT ( $p = 0.002$ ). ALT, alanine aminotransferase; AST, aspartate aminotransferase; ALP, alkaline phosphatase; GGT, gamma-glutamyl transferase

were removed for each biomarker, AUDs in the highest quartile of GGT levels exhibited increased EAA ( $b = 2.71$ ,  $p = 0.002$ ), as did individuals in the highest quartile of ALT levels ( $b = 2.19$ ,  $p = 0.007$ ) and ALP ( $b = 2.25$ ,  $p = 0.01$ ) in the basic model. When adjusted for all covariates in the full model, associations of age acceleration in elevated GGT, ALT, and ALP remained. Individuals with AUD who smoked exhibited a 1.77-year increase in age acceleration ( $p = 0.007$ ) compared to AUDs who did not smoke.

#### GWAS of epigenetic age acceleration

We first performed a GWAS of each AUD EA and AUD AA sample separately (Manhattan plots shown in Supplementary Figs. S1, S2), and then removed SNPs that had substantial heterogeneity between the GWAS results of EA and AA such as the flipping of the minor allele. The total number of SNPs for meta GWAS analysis was 494 067. We found no evidence for genomic inflation in each EA ( $\lambda_{GC} = 1.007$ ) and AA ( $\lambda_{GC} = 1.005$ ) studies. Interestingly, at a genome-wide significant level of  $P < 7.5 \times 10^{-8}$ , meta-analysis of

**Table 1.** Estimated marginal means of Levine's epigenetic age acceleration in AUD cases vs. controls

	AUD Cases (N = 331)				Controls (N = 201)				$\beta$	P-value
	Mean EAA	SE	95% CI		Mean EAA	SE	95% CI			
Levine (EPIC)										
Basic model	0.84	0.29	0.27	1.41	-1.38	0.39	-2.14	-0.62	2.22	<b>&lt;0.0001</b>
Full model	0.57	0.31	-0.04	1.18	-0.81	0.43	-1.66	0.04	1.38	<b>0.02</b>
Horvath 2013 (450K)										
Basic model	0.08	0.22	-0.34	0.51	-0.14	0.29	-0.71	0.43	0.22	0.56
Full model	0.22	0.23	-0.24	0.68	-0.25	0.33	-0.89	0.39	0.47	0.29
Hannum (450K)										
Basic model	-0.016	0.19	-0.38	0.35	0.03	0.25	-0.46	0.51	-0.04	0.9
Full model	0.09	0.2	-0.29	0.48	0.016	0.27	-0.52	0.55	0.07	0.83

Basic model adjusted for gender and blood cell-type composition. Full model adjusted for gender, blood cell-type composition, race (based on ancestry-informative marker score), smoking status, and body mass index. Levine PhenoAge Clock was designed for all three Illumina arrays (27k, 450k, and EPIC). Horvath and Hannum clocks were designed for 450K chip. Boldface indicates significance  
AUD alcohol use disorder

**Table 2.** Associations between Levine EAA and clinical characteristics in AUD cases (N = 331)

Predictor	Basic model		Full model	
	$\beta$	P-value	$\beta$	P-value
Heavy drinking days (highest/lowest quartile)	2.18	<b>0.01</b>	2.04	<b>0.02</b>
Elevated GGT	2.71	<b>0.002</b>	2.74	<b>0.001</b>
Elevated ALT	2.19	<b>0.007</b>	1.88	<b>0.03</b>
Elevated AST	1.06	0.22	1.43	0.11
Elevated ALP	2.25	<b>0.01</b>	1.92	<b>0.04</b>
Smoker	1.77	<b>0.007</b>	1.86	<b>0.005</b>

Adjusted for gender, blood cell-type composition in the basic model, and additionally adjusted for race, and body mass index in the full model for all outcome variables. Smoking status was also adjusted when examining heavy drinking days, GGT, ALT, AST, and ALP. Heavy drinking days are defined as  $\geq 4$  drinks a day for females;  $\geq 5$  drinks a day for males. AUD cases with the highest number of heavy drinking days (highest quartile) were compared to individuals with the lowest number of heavy drinking days (lowest quartile). Similarly, AUD cases with GGT, ALT, AST, and ALP levels in the highest quartile were compared to AUD cases with respective biomarker levels in the lowest quartile. AUD cases who smoke were compared to non-smoking cases. Boldface indicates significance  
AUD alcohol use disorder, GGT gamma-glutamyl transferase, ALT alanine aminotransferase, AST aspartate aminotransferase, ALP alkaline phosphatase

EAA showed that the SNP rs916264 in *APOL2* was significantly associated with an increase in EAA by 3.09 years ( $p = 5.4 \times 10^{-8}$ ) with each additional copy of the minor allele A (Fig. 2a, b, Table 3). None of the SNPs in each EA and AA GWAS was associated with EAA at the genome-wide significant level (Supplementary Figs. S1, S2). The top 20 SNPs in each EA and AA GWAS are presented in Supplementary Tables S3 and S4. Table 3 illustrates the top seven SNPs whose meta  $p$ -values were less than the suggestive significance level ( $P < 1 \times 10^{-5}$ ). The most significant SNP identified by the EA GWAS, rs2157250 in *APOL2* ( $p = 4.2 \times 10^{-7}$ ), was in high linkage disequilibrium (LD,  $R^2 = 0.6$ ) with rs916264 (Fig. 2b, Supplementary Table S3) and was also identified by the meta-analysis ( $p = 6.6 \times 10^{-7}$ ) with a moderate heterogeneity of 72.6%. Furthermore, each copy of major allele A of rs10043634 in *CWC27* was associated with a 3.21-year increases in EAA (meta  $p = 9.5 \times 10^{-6}$ ). Two SNPs, rs1327265 located 308kb away from

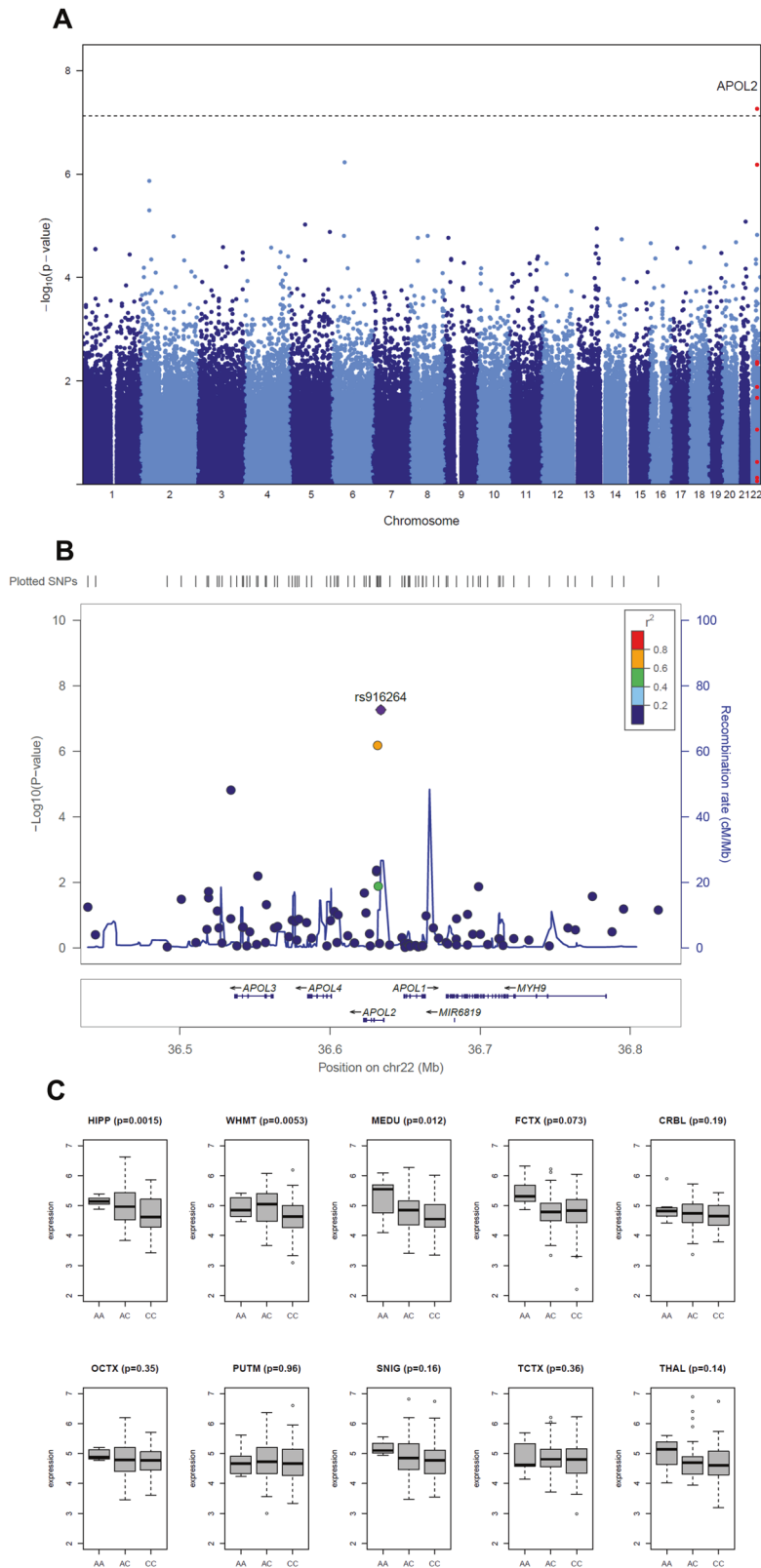
*PKHD1* and rs1571695 located 18kb away from *CLIC6*, showed suggestive association with EAA ( $p = 5.8 \times 10^{-7}$ ,  $8.4 \times 10^{-6}$ , respectively). Two additional SNPs, rs17014720 and rs2059442, in *LINC01317* also showed suggestive association and had high LD ( $R^2 = 1$  in CEU,  $R^2 = 0.93$  in ASW).

Cis-eQTL analysis on the BRAINEAC dataset showed that the genome-wide significant SNP rs916264 was positively correlated with brain mRNA expression across several brain regions (Fig. 2c). The minor allele A driving increased age acceleration had strongest associations with *APOL2* mRNA expression in the hippocampus ( $p = 0.0015$ ).

The gene set enrichment analysis by MAGENTA identified biological pathways among the pre-specified 20 biological processes targeting addition-, longevity-, or depression-related pathways from the KEGG pathway database (Supplementary Table S1). At the significant level of nominal  $p$ -values  $< 0.05$  and FDR-adjusted  $p$ -values  $< 0.2$ , the long-term depression pathway was detected to harbor more significant genes than expected ( $p = 0.0014$ , FDR  $p = 0.015$ ) by thresholding the MAGENTA  $p$ -value at the 95th percentile. In addition, three biological pathways (dopaminergic synapse, cAMP signaling pathway, mineral absorption) were nominally significant. None of the pathways were identified by thresholding the MAGENTA  $p$ -value at the 75th percentile.

## DISCUSSION

In this paper, we investigated epigenetic aging in individuals with AUD using data from the largest study of epigenetic aging in AUD to date. We also investigated the underlying biological mechanisms of age acceleration in AUD. Our study confirmed that epigenetic age acceleration, derived from Levine's DNAm PhenoAge algorithm, is increased in the AUD group compared to HC. However, we did not find significant associations of AUD status with age acceleration derived from the Horvath and Hannum epigenetic clocks, possibly due to differences in the methods capturing the age-related CpG sites. Furthermore, our exploratory analyses revealed more pronounced age acceleration in individuals with more severe AUD-associated phenotypes, such as elevated GGT, even when controlling for confounding factors. This implies that individuals with AUD with liver and/or tissue damage, as indicated by elevated liver enzymes, may experience accelerated aging and possibly shorter lifespans. To further elucidate the underlying molecular mechanisms and genetic factors contributing to epigenetic



aging in AUD, we conducted GWAS of epigenetic age acceleration in our sample and identified a genome-wide significant SNP, rs916264, located in an intronic region in *APOL2* on chromosome 22q12.3 which alters mRNA expression levels of *APOL2* in brain.

Our study significantly expands upon a previous study by Rosen et al., which found epigenetic aging in AUD and reported an association between epigenetic aging and excessive alcohol consumption in blood and liver [15]. In the current study, which employed more comprehensive analyses with well-characterized

**Fig. 2** GWAS of EAA identifies *APOL2*. **a** Manhattan plot shows the meta-analysis *P*-values combining the results of EA and AA AUD GWAS based on a fixed effect model using weight of inverse variance. EA and AA studies comprised of 154 AUD EA and 156 AUD AA individuals. The y-axis reports log transformed meta *P*-values. The horizontal dashed line corresponds to the genome-wide association threshold ( $p = 7.5 \times 10^{-8}$ ). All SNPs in *APOL2* were colored with red. **b** Regional association plot of *APOL2* associated with epigenetic age acceleration. The y-axis shows the log-transformed meta-analysis *P*-value. The colors represent linkage disequilibrium (LD)  $R^2$ . **c** Association of rs916264 genotype with *APOL2* mRNA exon specific expression in the 10 brain tissues (Affymetrix Expression ID = 3959439). The y-axis is a log2 transformed expression scale. The x-axis describes the genotype group of rs916264 across the 10 brain tissues. HIPP stands for hippocampus, WHMT for intralobular matter, MEDU for medulla (specifically inferior olivary), FCTX for frontal cortex, CRBL for cerebella cortex, OCTX for occipital cortex (specifically primary visual cortex), PUTM for putamen, SNIG for substantia nigra, TCTX for temporal cortex, THAL for thalamus

**Table 3.** GWAS meta-analysis of EAA in EA and AA AUD case (listed by  $p < 1 \times 10^{-5}$ )

SNP	CHR	BP	Minor/Major allele	EA		AA		META			Gene or nearest gene
				MAF	<i>P</i> -value	MAF	<i>P</i> -value	BETA (EFFECT)	<i>P</i> -value	$I^2$ (P)	
rs916264	22	36633836	A <sup>a</sup> /C	0.26	2.07E-06	0.04	0.025	3.09	5.43E-08	0 (0.92)	<i>APOL2</i>
rs1327265	6	51171408	G/A <sup>a</sup>	0.39	0.0039	0.30	5.18E-05	2.17	5.84E-07	2.01 (0.31)	308kb away from <i>PKHD1</i>
rs2157250	22	36631691	G <sup>a</sup> /A	0.25	4.21E-07	0.09	0.60	2.70	6.61E-07	72.6 (0.06)	<i>APOL2</i>
rs17014720	2	34328691	C/T <sup>a</sup>	0.17	0.00015	0.20	0.0045	2.45	1.34E-06	0 (0.75)	<i>LINC01317</i>
rs2059442	2	34324360	C/T <sup>a</sup>	0.17	0.00053	0.20	0.0045	2.34	5.00E-06	0 (0.90)	<i>LINC01317</i>
rs1571695	21	36023355	C/A <sup>a</sup>	0.35	0.00190	0.27	0.0019	1.99	8.37E-06	0 (0.66)	18kb away from <i>CLIC6</i>
rs10043634	5	64118974	G/A <sup>a</sup>	0.09	0.00083	0.10	0.0055	3.21	9.51E-06	0 (0.98)	<i>CWC27</i>

*P*-value present refers to association test with EAA

EA European Ancestry participants, AA Africa Ancestry participants, META GWAS meta-analysis, CHR chromosome, BP base pair (physical location) on genome, MAF minor allele frequency, *APOL2* Apolipoprotein L2, *PKHD1* PKHD1 ciliary IPT domain containing fibrocystin/polyductin, *LINC01317* Long intergenic non-protein coding RNA 1317, *CLIC6* Chloride Intracellular Channel 6, *CWC27* Spliceosome Associated Protein Homolog,  $I^2$  (P) heterogeneity index with *P*-value  
<sup>a</sup>In minor/major allele shows the allele drives the epigenetic age acceleration (i.e., each copy of a minor allele A in rs916264 increases EAA by 3.09)

alcohol consumption-related phenotypes and endophenotypes of liver function test enzymes, we utilized the Levine DNAm PhenoAge epigenetic clock as well as Hannum and Horvath's epigenetic clocks. Interestingly, our findings of EAA in AUD and its associated endophenotypes were found using only Levine's epigenetic clock. The Levine clock was previously shown to better differentiate morbidity and mortality risk among individuals of the same chronological age than other epigenetic clocks [12]. Although the present study examined methylation in whole blood only, we controlled for pertinent factors (e.g., blood cell-type composition) that the previous study by Rosen et al. did not. These factors have been shown to significantly impact variability in DNA methylation and are likely influenced by heavy alcohol consumption [26, 34]. One possible explanation for the failure to replicate the finding of Rosen et al.'s (2018) using Horvath's epigenetic clock is that first-generation clocks were designed for Illumina's 450k DNA methylation array. There have been mixed findings on whether DNAm-based estimations from first-generation clocks are accurate when using the EPIC array [35, 36]. DNAm age estimated by the first-generation approaches in our cohort could be inaccurate due to missing probes between the arrays, despite probe imputation procedures [36]. Furthermore, Levine's second-generation clock has been found to be more strongly associated with alcohol intake and smoking compared with first-generation clocks [7], which could indicate that different clocks capture different aspects of epigenetic aging. Our finding of age acceleration in individuals with AUD using Levine's approach but not Horvath's or Hannum's is not unexpected because Levine's clock was designed to include CpG sites associated with biomarkers of physiological dysregulation and chronic diseases. In contrast, the Horvath and Hannum clocks include CpGs that predict chronological age only.

We further employed the Levine clock to understand how the severity of AUD phenotype, characterized by drinking pattern and clinical biomarkers of alcohol use, is associated with epigenetic aging. We found that the most severe AUD (i.e., individuals in the

highest quartile for number of drinking days and levels of liver enzymes) exhibited on average greater age acceleration than the least severe AUD cases in the lowest quartile for these clinical characteristics. Our results provide evidence that within AUD populations, clinical heterogeneity could lead to differences in future morbidity and point to the possibility of uncovering shared mechanisms of AUD with aging-related morbidity. We examined the effects of heavy drinking days and liver enzyme levels using both the basic, minimally adjusted model, as well as the full model adjusting for all covariates. Here, we did not observe significant differences in age acceleration between the two models, which supports the robustness of our findings.

Epigenetic clocks have been employed to study age acceleration in other neuropsychiatric disorders in addition to AUD. In major depressive disorder, patients with depression experience a 0.64-year increase in EAA after adjusting for sex, education level, body mass index, cotinine levels, alcohol use, physical activity, and number of chronic diseases [37]. A study investigating post-traumatic stress disorder (PTSD) among veterans found a 1.97-year increase in EAA in individuals exhibiting PTSD symptoms, but the study is limited by a small sample size of 96 [38]. Both studies used blood to obtain methylation levels. Mixed results have been seen in schizophrenia. One study found no accelerated aging in the brain or blood of schizophrenia patients [39]. Another study reported a decrease in age acceleration in the blood of schizophrenia patients in one cohort but no effect in another [40]. To the best of our knowledge, no studies have been done on epigenetic aging in individuals with substance use disorders. Our finding of a 1.38-year age acceleration (full model) in AUD is significant as our effect size is the same as or greater than EAA in other neuropsychiatric disorders. It is interesting that a similar range of EAA is observed across psychiatric disorders, as psychiatric comorbidity is common and cross-disorder genetic susceptibility has previously been suggested [41]. One possible speculation could be that shared genetic or epigenetic susceptibility could also play a role in biological aging in these psychiatric disorders.

Given that DNA methylation is sensitive to both genetic and environmental factors, our findings do not determine whether DNA methylation differences and epigenetic age acceleration are predisposing factors for addiction or if they are consequences of long-term alcohol use. To address this limitation of our cross-sectional case-control study, future studies may collect methylation data from multiple time points to investigate how substance exposure and epigenetic aging interact. It would be beneficial to determine whether epigenetic age acceleration can be a biomarker that tracks changes in drinking patterns over time and whether the removal of harmful factors like chronic, heavy alcohol consumption can decelerate aging. Furthermore, although methylation, and thus epigenetic aging, in peripheral blood and brain has been shown to be highly correlated [8, 42], future studies should confirm the association between EAA in the blood or EAA derived from postmortem brain tissue. Our study was also limited in the covariates representing environmental factors that were not available to include in the analyses. While we accounted for gender, blood-cell composition, BMI, race, and smoking status, we did not collect data on other environmental factors that can impact DNA methylation levels and epigenetic aging. Covariates such as exercise, diet, and environmental toxin exposure, like air pollution, which have been shown to impact epigenetic aging should be included in future studies with larger sample sizes [25, 43].

In order to investigate the genetic contributing factors underlying EAA in AUD, we conducted GWAS analyses and identified in our meta-analysis, a genome-wide significant SNP, rs916264 in the gene encoding apolipoprotein L2 (*APOL2*). The apolipoprotein family of proteins facilitate the transport of lipids and lipophilic substrates [44]. *APOL2* is related to cholesterol biosynthesis and trafficking and has been suggested to mediate cell death induced by interferon-gamma or viral infection. However, the role of *APOL2* in cell death remains unclear [45]. Moreover, differential expression of *APOL2* has been observed in individuals with substance use disorders (cocaine, cannabis, and phencyclidine) [46] as well as schizophrenia and bipolar disorders [47]. *APOL2* is highly expressed in several brain regions. The BRAINEAC dataset confirmed that the top significant variant, rs916264, is significantly associated with expression of *APOL2* in the hippocampus as well as in intralobular white matter and the medulla. Among the three brain regions, the hippocampus showed the strongest correlation with rs916264 genotype. This suggests rs916264 may influence regulation of *APOL2* expression in human hippocampus. However, the biological function of *APOL2* in the brain remains unclear [44, 46]. Furthermore, three SNPs in *LINC01317* and *CWC27* showed suggestive association with EAA. *LINC01317* is a non-protein coding RNA that is transcribed from DNA but not translated into proteins and is generally associated with regulation of gene expression. To date, no study has published on the gene. *CWC27* plays a role in pre-mRNA splicing and codes for a cyclophilin, which is part of the spliceosome and has been implicated in retinal degeneration, including age-related macular degeneration [48–50].

To the best of our knowledge, our study was the first GWAS analysis of epigenetic age acceleration in an AUD population. Previous GWAS on age acceleration have been done in brain and blood and have implicated genes coding for telomerase reverse transcriptase as well as loci (17q11.2 and 1p36.12) associated with the expression levels of multiple genes including *EFCAB5*, involved in calcium ion binding, and *CRLF3*, which regulates cell cycle progression [51, 52]. Our GWAS analysis identified several other variants whose effects are mild to moderate but did not meet a statistically significant genome-wide threshold after correcting for multiple comparisons. These variants are usually polygenic, meaning they could be related to functionally relevant biological pathways.

Using either top 5% or 25% significant genetic variants, our gene set enrichment analysis compared our results of GWAS analysis with sets of genes in pre-specified pathways that are relevant with aging or addiction. Our top 5% findings were enriched in a set of genes involved in a pathway of cerebellar long-term depression, a process involving the reduction in synaptic strength between parallel fiber and Purkinje cell [53]. This finding may be significant as acute alcohol consumption has been shown to suppress parallel fiber long-term depression in the cerebellum, which may contribute to alcohol-induced deficits in motor coordination in rats [54, 55]. Furthermore, in mice, chronic alcohol consumption has been shown to impair the sensory stimulation-induced molecular layer interneurons (MLIs) to the Purkinje cell (PC) synapses through the activation of a nitric oxide signaling pathway in the cerebellar cortex, which could lead to a deficit in cerebellar motor learning [56]. Taken together, our findings suggest that chronic alcohol abuse in AUD individuals may impact cerebellar long-term depression, which could have pleiotropic effects leading to accelerated biological aging.

In addition, we found three biological pathways (dopaminergic synapse, cAMP signaling, and mineral absorption) to be nominally significant using the KEGG Pathway database. The dopaminergic synapse pathway includes components of the dopaminergic signaling, including its five receptors (D1, D2, D3, D4, and D5). The dopaminergic reward system has been implicated in alcohol dependence as well as other substance use disorders, such as cocaine dependence [57]. Specifically, there is evidence for the association between genetic variation in the D2 dopamine receptor gene (*DRD2*) and alcoholism [57, 58]. The *TaqI* A minor (A1) allele of the *DRD2* gene reduces the number of D2 dopamine receptors in the brain, reducing the efficiency of the dopaminergic system [57]. It is hypothesized that abuse of substances like alcohol may increase brain dopamine levels. Furthermore, animal studies have shown that drugs of abuse increase extracellular dopamine in the nucleus accumbens [58]. This pathway has also been implicated in other neuropsychiatric disorders including obsessive-compulsive disorder, schizophrenia, and attention deficit hyperactivity disorder [59–61]. The cAMP signaling pathway includes cAMP, one of the most common second messengers, adenylyl cyclase (AC), G protein-coupled receptors, protein kinase A (PKA), and other components. This finding is of interest as alcohol and other drugs of abuse have been shown to affect cAMP-PKA signaling in the mesolimbic pathway [62]. Acute alcohol consumption has been shown to elevate extracellular adenosine levels, which plays a role in mediating alcohol preference and its sedative effects [63]. Furthermore, alcohol has been suggested to stimulate AC activity, with a positive family history of alcohol dependence being associated with higher levels of AC activity [64]. Lastly, the mineral absorption pathway consists of the passive or active transport systems that help absorb minerals and transport proteins. Alcohol is known to disrupt osteoblastic activity, which results in decreased bone formation and impaired mineralization [65]. Heavy alcohol use has been associated with decreased bone mineral density and impairs bone remodeling, leading to bone loss and increased risk for osteoporosis and fracture [66–68]. This pathway plays a role in bone diseases such as osteoporosis and may suggest the role of disrupted mineral absorption in AUD that could lead to accelerated aging [69]. While these pathways did not reach statistical significance after correction for multiple comparisons, there is evidence of their potential roles in the relationship between aging and AUD. Future studies with larger sample sizes may further explore these biological pathways.

Our study is the largest epigenetic aging study of AUD to date and was adequately powered to detect EAA with 80% power to identify an age acceleration difference of 1.5–2 years between AUD and healthy controls at the 1–5% significance level. Our GWAS of epigenetic aging in AUD would benefit from a larger

sample size that would allow the detection of additional variants with stronger significance due to higher statistical power. Our GWAS of EAA focused on and analyzed only common variants with minor allele frequencies greater than 1% that were available in both of the Illumina OmniExpress BeadChips. Detection of rare genetic variants requires a larger sample size. We may also miss rare functional variants with large effects, which could influence EAA. Finally, future studies of epigenetic aging in AUD might consider high-throughput interrogation of a genome-wide study.

In conclusion, our study indicates accelerated biological aging in individuals with AUD and more pronounced acceleration in individuals with more severe clinical AUD phenotypes. In addition, we identified an association between *APOL2* and EAA in AUD, suggesting a potential role of apolipoproteins in molecular aging. Our findings warrant further investigation into the shared mechanisms underlying AUD and aging, which can lead to the development of novel methods of detection and treatment for aging-related morbidities.

## FUNDING AND DISCLOSURE

This work was supported by the National Institutes of Health (NIH) intramural funding [ZIA-AA000242 to F.W.L.]; Division of Intramural Clinical and Biological Research of the National Institute on Alcohol Abuse and Alcoholism (NIAAA). The authors declare no competing interests.

## ADDITIONAL INFORMATION

**Supplementary Information** accompanies this paper at (<https://doi.org/10.1038/s41386-019-0500-y>).

**Publisher's note:** Springer Nature remains neutral with regard to jurisdictional claims in published maps and institutional affiliations.

## REFERENCES

1. Saieva C, Bardazzi G, Masala G, Quartini A, Ceroti M, Iozzi A, et al. General and cancer mortality in a large cohort of Italian alcoholics. *Alcohol Clin Exp Res* 2012;36:342–50.
2. Udo T, Vasquez E, Shaw BA. A lifetime history of alcohol use disorder increases risk for chronic medical conditions after stable remission. *Drug Alcohol Depend*. 2015;157:68–74.
3. Griswold MG, Fullman N, Hawley C, Arian N, Zimsen SRM, Tymeson HD, et al. Alcohol use and burden for 195 countries and territories, 1990–2016: a systematic analysis for the Global Burden of Disease Study 2016. *Lancet*. 2018;392:1015–35.
4. Westman J, Wahlbeck K, Laursen TM, Gissler M, Nordentoft M, Hallgren J, et al. Mortality and life expectancy of people with alcohol use disorder in Denmark, Finland and Sweden. *Acta Psychiatr Scand*. 2015;131:297–306.
5. Laramée P, Leonard S, Buchanan-Hughes A, Warnakula S, Daeppen J-B, Rehm J. Risk of all-cause mortality in alcohol-dependent individuals: a systematic literature review and meta-analysis. *EBioMedicine*. 2015;2:1394–404.
6. Beach SRH, Dogan MV, Lei M-K, Cutrona CE, Gerrard M, Gibbons FX, et al. Methylomic aging as a window onto the influence of lifestyle: tobacco and alcohol use alter the rate of biological aging. *J Am Geriatr Soc*. 2015;63:2519–25.
7. Fiorito G, McCrory C, Robinson O, Carmeli C, Rosales CO, Zhang Y, et al. Socio-economic position, lifestyle habits and biomarkers of epigenetic aging: a multi-cohort analysis. *Aging (Albany NY)*. 2019;11:2045–70.
8. Horvath S. DNA methylation age of human tissues and cell types. *Genome Biol*. 2013;14:R115.
9. Zhang H, Gelernter J. Review: DNA methylation and alcohol use disorders: Progress and challenges. *Am J Addict*. 2017;26:502–15.
10. Lohoff FW, Sorcher JL, Rosen AD, Mauro KL, Fanelli RR, Momenan R, et al. Methylomic profiling and replication implicates deregulation of PCSK9 in alcohol use disorder. *Mol Psychiatry*. 2018;23:1–11.
11. Zhang H, Herman AI, Kranzler HR, Anton RF, Zhao H, Zheng W, et al. Array-based profiling of DNA methylation changes associated with alcohol dependence. *Alcohol Clin Exp Res*. 2013;37(Suppl 1):E108–15.
12. Levine ME, Lu AT, Quach A, Chen BH, Assimes TL, Bandinelli S, et al. An epigenetic biomarker of aging for lifespan and healthspan. *Aging (Albany NY)* 2018;10:573–91.
13. Horvath S, Oshima J, Martin GM, Lu AT, Quach A, Cohen H, et al. Epigenetic clock for skin and blood cells applied to Hutchinson Gilford Progeria Syndrome and ex vivo studies. *Aging (Albany NY)* 2018;10:1758–75.
14. Hannum G, Guinney J, Zhao L, Zhang L, Hughes G, Sada S, et al. Genome-wide methylation profiles reveal quantitative views of human aging rates. *Mol Cell*. 2013;49:359–67.
15. Rosen AD, Robertson KD, Hlady RA, Muench C, Lee J, Philibert R, et al. DNA methylation age is accelerated in alcohol dependence. *Transl Psychiatry*. 2018;8:182.
16. Levine ME, Hosgood HD, Chen B, Absher D, Assimes T, Horvath S. DNA methylation age of blood predicts future onset of lung cancer in the women's health initiative. *Aging*. 2015;7:690–700.
17. Marioni RE, Shah S, McRae AF, Chen BH, Colicino E, Harris SE, et al. DNA methylation age of blood predicts all-cause mortality in later life. *Genome Biol*. 2015;16:25.
18. Goldstein RB, Chou SP, Smith SM, Jung J, Zhang H, Saha TD, et al. Nosologic comparisons of DSM-IV and DSM-5 alcohol and drug use disorders: results from the National Epidemiologic Survey on Alcohol and Related Conditions–III. *J Stud Alcohol Drugs*. 2015;76:378–88.
19. Sobell LC, Sobell MB. Timeline Follow-Back. In: Litten RZ, Allen JP, editors. *Measuring Alcohol Consumption: Psychosocial and Biochemical Methods*. Totowa, NJ: Humana Press; 1992. p. 41–72.
20. Heatherton TF, Kozlowski LT, Frecker RC, Fagerstrom KO. The fagerstrom test for nicotine dependence: a revision of the fagerstrom tolerance questionnaire. *Br J Addict*. 1991;86:1119–27.
21. Kuan PF, Wang S, Zhou X, Chu H. A statistical framework for Illumina DNA methylation arrays. *Bioinformatics*. 2010;26:2849–55.
22. Houseman EA, Kile ML, Christiani DC, Ince TA, Kelsey KT, Marsit CJ. Reference-free deconvolution of DNA methylation data and mediation by cell composition effects. *BMC Bioinforma*. 2016;17:259.
23. Horvath S, Gurven M, Levine ME, Trumble BC, Kaplan H, Allayee H, et al. An epigenetic clock analysis of race/ethnicity, sex, and coronary heart disease. *Genome Biol*. 2016;17:171.
24. DiFranza JR, Guerrera MP. Alcoholism and smoking. *J Stud Alcohol*. 1990; 51:130–5.
25. Quach A, Levine ME, Tanaka T, Lu AT, Chen BH, Ferrucci L, et al. Epigenetic clock analysis of diet, exercise, education, and lifestyle factors. *Aging (Albany NY)*. 2017;9:419–46.
26. Jaffe AE, Irizarry RA. Accounting for cellular heterogeneity is critical in epigenome-wide association studies. *Genome Biol*. 2014;15:R31.
27. Hattab MW, Shabalini AA, Clark SL, Zhao M, Kumar G, Chan RF, et al. Correcting for cell-type effects in DNA methylation studies: reference-based method outperforms latent variable approaches in empirical studies. *Genome Biol*. 2017;18:24.
28. Wiers CE, Towb PC, Hodgkinson CA, Shen PH, Freeman C, Miller G, et al. Association of genetic ancestry with striatal dopamine D2/D3 receptor availability. *Mol Psychiatry*. 2018;23:1711–6.
29. Rosenberg NA, Pritchard JK, Weber JL, Cann HM, Kidd KK, Zhivotovskiy LA, et al. Genetic structure of human populations. *Science*. 2002;298:2381.
30. Segrè AV, Consortium D, investigators M, Groop L, Mootha VK, Daly MJ, et al. Common inherited variation in mitochondrial genes is not enriched for associations with type 2 diabetes or related glycemic traits. *PLoS Genet*. 2010;6: e1001058.
31. Kanehisa M, Sato Y, Furumichi M, Morishima K, Tanabe M. New approach for understanding genome variations in KEGG. *Nucleic Acids Res*. 2018;47(D1): D590–D5.
32. Uhlén M, Fagerberg L, Hallström BM, Lindskog C, Oksvold P, Mardinoglu A, et al. Tissue-based map of the human proteome. *Science*. 2015;347:1260419.
33. Ramasamy A, Trabzuni D, Guelfi S, Varghese V, Smith C, Walker R, et al. Genetic variability in the regulation of gene expression in ten regions of the human brain. *Nat Neurosci*. 2014;17:1418.
34. Ballard HS. The hematological complications of alcoholism. *Alcohol Health Res World*. 1997;21:42–52.
35. McEwen LM, Jones MJ, Lin DTS, Edgar RD, Husquin LT, Maclsaac JL, et al. Systematic evaluation of DNA methylation age estimation with common preprocessing methods and the Infinium MethylationEPIC BeadChip array. *Clin Epigenetics*. 2018;10:123.
36. Dhingra R, Kwee LC, Diaz-Sanchez D, Devlin RB, Cascio W, Hauser ER, et al. Evaluating DNA methylation age on the Illumina MethylationEPIC Bead Chip. *PLoS One*. 2019;14:e0207834.
37. Han LKM, Aghajani M, Clark SL, Chan RF, Hattab MW, Shabalini AA, et al. Epigenetic Aging in Major Depressive Disorder. *Am J Psychiatry*. 2018;175:774–82.
38. Boks MP, van Mierlo HC, Rutten BP, Radstake TR, De Witte L, Geuze E, et al. Longitudinal changes of telomere length and epigenetic age related to traumatic stress and post-traumatic stress disorder. *Psychoneuroendocrinology*. 2015;51:506–12.

39. McKinney BC, Lin H, Ding Y, Lewis DA, Sweet RA. DNA methylation age is not accelerated in brain or blood of subjects with schizophrenia. *Schizophr Res*. 2018;196:39–44.
40. Okazaki S, Otsuka I, Numata S, Horai T, Mouri K, Boku S, et al. Epigenetic clock analysis of blood samples from Japanese schizophrenia patients. *NPJ Schizophr*. 2019;5:4.
41. Walters RK, Polimanti R, Johnson EC, McClintick JN, Adams MJ, Adkins AE, et al. Transancestral GWAS of alcohol dependence reveals common genetic underpinnings with psychiatric disorders. *Nat Neurosci*. 2018;21:1656–69.
42. Tylee DS, Kawaguchi DM, Glatt SJ. On the outside, looking in: a review and evaluation of the comparability of blood and brain "-omes". *Am J Med Genet B Neuropsychiatr Genet*. 2013;162B:595–603.
43. Ward-Caviness CK, Nwanaji-Enwerem JC, Wolf K, Wahl S, Colicino E, Trevisi L, et al. Long-term exposure to air pollution is associated with biological aging. *Oncotarget*. 2016;7:74510–25.
44. Elliott DA, Weickert CS, Garner B. Apolipoproteins in the brain: implications for neurological and psychiatric disorders. *Clin Lipidol*. 2010;5:1555–73.
45. Galindo-Moreno J, Iurlaro R, El Mjiyad N, Diez-Perez J, Gabaldon T, Munoz-Pinedo C. Apolipoprotein L2 contains a BH3-like domain but it does not behave as a BH3-only protein. *Cell Death Dis*. 2014;5:e1275.
46. Lehmann E, Colantuoni C, Deep-Soboslay A, Becker KG, Lowe R, Huestis MA, et al. Transcriptional changes common to human cocaine, cannabis and phenylcyclidine abuse. *PLoS One*. 2006;1:e114.
47. Takahashi S, Cui YH, Han YH, Fagerness JA, Galloway B, Shen YC, et al. Association of SNPs and haplotypes in APOL1, 2 and 4 with schizophrenia. *Schizophr Res*. 2008;104:153–64.
48. Wang M, Li Z, Chu H, Lv Q, Ye D, Ding Q, et al. Genome-wide association study of bladder cancer in a Chinese Cohort reveals a new susceptibility locus at 5q12.3. *Cancer Res*. 2016;76:3277–84.
49. Ma D, Yang J, Wang Y, Huang X, Du G, Zhou L. Whole exome sequencing identified genetic variations in Chinese hemangioblastoma patients. *Am J Med Genet A*. 2017;173:2605–13.
50. Xu M, Xie YA, Abouzeid H, Gordon CT, Fiorentino A, Sun Z, et al. Mutations in the spliceosome component CWC27 cause retinal degeneration with or without additional developmental anomalies. *Am J Hum Genet* 2017;100:592–604.
51. Lu AT, Hannon E, Levine ME, Crimmins EM, Lunnon K, Mill J, et al. Genetic architecture of epigenetic and neuronal ageing rates in human brain regions. *Nat Commun*. 2017;8:15353.
52. Lu AT, Xue L, Salfati EL, Chen BH, Ferrucci L, Levy D, et al. GWAS of epigenetic aging rates in blood reveals a critical role for TERT. *Nat Commun*. 2018;9:387.
53. Hirano T. Long-term depression and other synaptic plasticity in the cerebellum. *Proc Jpn Acad Ser B Phys Biol Sci*. 2013;89:183–95.
54. Belmeuguenai A, Botta P, Weber JT, Carta M, De Ruiter M, De Zeeuw CI, et al. Alcohol impairs long-term depression at the cerebellar parallel fiber-Purkinje cell synapse. *J Neurophysiol* 2008;100:3167–74.
55. Su LD, Sun CL, Shen Y. Ethanol acutely modulates mGluR1-dependent long-term depression in cerebellum. *Alcohol Clin Exp Res* 2010;34:1140–5.
56. Li D-Y, Bing Y-H, Chu C-P, Cui X, Cui S-B, Qiu D-L, et al. Chronic ethanol consumption impairs the tactile-evoked long-term depression at cerebellar molecular layer interneuron-purkinje cell synapses in vivo in mice. *Front Cell Neurosci*. 2019;12:521.
57. Noble EP. Addiction and its reward process through polymorphisms of the D2 dopamine receptor gene: a review. *Eur Psychiatry*. 2000;15:79–89.
58. Di Chiara G, Bassareo V, Fenu S, De Luca MA, Spina L, Cadoni C, et al. Dopamine and drug addiction: the nucleus accumbens shell connection. *Neuropharmacology*. 2004;47(Suppl 1):227–41.
59. Kustanovich V, Ishii J, Crawford L, Yang M, McGough JJ, McCracken JT, et al. Transmission disequilibrium testing of dopamine-related candidate gene polymorphisms in ADHD: confirmation of association of ADHD with DRD4 and DRD5. *Mol Psychiatry*. 2004;9:711–7.
60. Cacabelos R, Martinez-Bouza R. Genomics and pharmacogenomics of schizophrenia. *CNS Neurosci Ther*. 2011;17:541–65.
61. Millet B, Chabane N, Delorme R, Leboyer M, Leroy S, Poirier MF, et al. Association between the dopamine receptor D4 (DRD4) gene and obsessive-compulsive disorder. *Am J Med Genet B Neuropsychiatr Genet*. 2003;116B:55–9.
62. Wand G, Levine M, Zweifel L, Schwindinger W, Abel T. The cAMP-protein kinase A signal transduction pathway modulates ethanol consumption and sedative effects of ethanol. *J Neurosci*. 2001;21:5297–303.
63. Ruby CL, Adams CA, Knight EJ, Nam HW, Choi DS. An essential role for adenosine signaling in alcohol abuse. *Curr Drug Abuse Rev*. 2010;3:163–74.
64. Peterson K. Biomarkers for alcohol use and abuse—a summary. *Alcohol Res Health*. 2004;28:30–7.
65. Rico H. Alcohol and bone disease. *Alcohol Alcohol*. 1990;25:345–52.
66. Turner RT. Skeletal response to alcohol. *Alcohol Clin Exp Res*. 2000;24:1693–701.
67. Gaddini GW, Turner RT, Grant KA, Iwaniec UT. Alcohol: a simple nutrient with complex actions on bone in the adult skeleton. *Alcohol Clin Exp Res*. 2016;40:657–71.
68. Cho Y, Choi S, Kim K, Lee G, Park SM. Association between alcohol consumption and bone mineral density in elderly Korean men and women. *Arch Osteoporos*. 2018;13:46.
69. Masi L, Becherini L, Colli E, Gennari L, Mansani R, Falchetti A, et al. Polymorphisms of the calcitonin receptor gene are associated with bone mineral density in postmenopausal Italian women. *Biochem Biophys Res Commun*. 1998;248:190–5.



**Open Access** This article is licensed under a Creative Commons Attribution-NonCommercial-NoDerivatives 4.0 International License, which permits any non-commercial use, sharing, distribution and reproduction in any medium or format, as long as you give appropriate credit to the original author(s) and the source, and provide a link to the Creative Commons license. You do not have permission under this license to share adapted material derived from this article or parts of it. The images or other third party material in this article are included in the article's Creative Commons license, unless indicated otherwise in a credit line to the material. If material is not included in the article's Creative Commons license and your intended use is not permitted by statutory regulation or exceeds the permitted use, you will need to obtain permission directly from the copyright holder. To view a copy of this license, visit <http://creativecommons.org/licenses/by-nc-nd/4.0/>.

© The Author(s) 2019